sciendo

POLISH MARITIME RESEARCH 3 (127) 2025 Vol. 32; pp. 33-46
10.2478/pomr-2025-0034

A COMPARATIVE STUDY OF BIOMIMICRY-INSPIRED DESIGN FORMS FOR AUTONOMOUS UNDERWATER VEHICLES

Mesut Taner
Bursa Technical University – Faculty of Maritime Department of Naval Architecture
and Marine Engineering Department of Naval Architect; Bursa; Turkey
Kadri Turgut Gürsel*
Dokuz Eylül University, Institute of Marine Sciences and Technology, Department of Naval Architect; Izmir; Turkey

* Corresponding author: *turgut.gursel@deu.edu.tr (Kadri Turgut Gürsel)*

ABSTRACT

Industrial development and surveying projects related to oil and natural gas resources and undersea pipelines require comprehensive geological, geophysical, and oceanographic research to be conducted in offshore and coastal areas. These research activities are typically conducted by research vessels or smaller craft that are specially equipped for specific tasks, which often require considerable labour. However, this research method incurs high operating costs and poses risks to occupational safety and property, particularly due to the harsh weather conditions at sea. In addition, high-precision measurements cannot always be effectively taken using these vessels at the sea surface during such projects. Consequently, research institutions and organisations have made significant advancements in developing autonomous underwater vehicles (AUVs) over the past two decades.

The aim of this study was to identify an optimal design form for AUVs to enable them to examine the geomorphological, geological, and geophysical structures of the seafloor while also supporting oceanographic research. To achieve this, computational fluid dynamics analyses were conducted on the DARPA (Defense Advanced Research Projects Agency) Suboff submarine model, and the results were validated using experimental data obtained from the literature [1]. After successfully confirming the accuracy of the simulations, which were executed using the commercial software STAR CCM+ (Simulation of Turbulent Flow in Arbitrary Regions - Computational Continuum Mechanics, C++ based), various AUV designs were created based on commonly used geometric shapes for torpedoes. In addition, biomimicry principles were employed to develop AUV models with minimal viscous resistance and energy consumption during underwater operations. The following models, all with the same displacement, were systematically analysed: a mature goose-beaked whale (Ziphius cavirostris), a mature sperm whale (Physeter macrocephalus), an adapted form of the submarine shark (Carcharodon carcharias, also known as the great white shark), four biomimicry-inspired hybrid models and four torpedo-shaped AUVs. The findings from these analyses are discussed in detail.

Keywords: Form development, Biomimicry, Autonomous underwater vehicle, CFD analysis, Marine research

INTRODUCTION

Development and surveying projects related to oil and natural gas resources, including underwater pipelines, involve tasks that need to be carried out in harbours, coastal, and offshore structures. These processes require geological and geophysical studies, as well as oceanographic research, and are typically conducted using research vessels, necessitating significant human effort. This approach has several drawbacks, such as high operational costs and problems with the accuracy of the measurements. In addition, prolonged research periods are common due to harsh marine conditions, and ship voyages under these conditions pose serious risks to the safety of both life and property at sea. Thus, over the past two decades, universities and research communities have made significant advancements in developing autonomous underwater vehicles (AUVs). These vehicles provide a valuable means of gathering detailed oceanographic, geological, geophysical, and seismic data directly from the field [2].

To meet the performance requirements of AUVs, the key design features include a low viscous resistance, high propulsive efficiency, and excellent manoeuvrability and navigational capabilities. To enhance the efficiency of the propulsion system, it is important to include propellers equipped with nozzles. A crucial factor in determining the operational route and duration of an AUV is an accurate prediction of the hull resistance, which is needed to calculate the power requirements. To estimate the power requirements effectively, it is essential to analyse the hull resistance carefully during the design phase and decide on a suitable power system based on the results [2-4]. The form features and operational depth of a vehicle significantly influence the power needed for underwater operations, as energy is consumed by AUVs both during forward movement and while maintaining a constant depth.

The design of various AUVs, particularly regarding hull resistance, propulsion efficiency, and other hydrodynamic properties, has been studied through both computational fluid dynamics (CFD) methods and experimental tests. Numerous articles have addressed these aspects, and some well-known studies are reviewed here.

In one study by Myring [3], data from the Royal Aviation Association were used to validate the results of a numerical analysis for various hull forms. In this research, a method was developed to determine the resistance of a hull form subjected to axisymmetric flow [2]. To effectively apply this method, it is essential to carefully identify certain key parameters, including the geometry of the hull form, flow conditions, and transition points.

In his book, Joubert [4] discussed some principles for enhancing the hydrodynamic properties of submarines. He introduced a new bow design with the aim of improving passive sonar performance at various operating speeds while also demonstrating the potential to reduce other significant sources of resistance. Bertram [5] outlined the general principles used in design and some solutions for submarine hulls and their appendages in his monograph.

Research conducted by Madhan et al. [6] provided a detailed analysis of the hydrodynamic hull design, resistance, and propulsion characteristics of a torpedo-shaped AUV named MAYA. Joung et al. [7] carried out CFD simulations to predict hull resistance as part of the development of an AUV design. Their study also addressed the optimisation of the AUV hull profile to reduce the overall resistance, and demonstrated that form optimisation is achievable during the conceptual design phase using commercial CFD software. In addition, Husaini et al. [8] examined the resistance force behaviour of AUVs using CFD methodology, focusing on two different operating positions for AUVs working in groups in order to analyse the changes in resistance. Their findings indicated that the distance behind the leading AUV has a minimal impact on the resistance force when the vehicles travel in tandem, but that it is essential to regulate their positions to effectively manage this force.

Karim et al. [9] conducted numerical analyses of a series of AUV models known as DREA, using the finite volume method based on the Reynolds-averaged Navier-Stokes (RANS) equations to assess their viscous resistances. This model series comprised six axially symmetrical hulls, with length-to-diameter ratios ranging from four to 10. The study focused on examining the turbulent flows around and behind the hulls, using the shear stress transport (SST) k-ω turbulence algorithm. Similarly, Fangxi et al. [10] identified suitable turbulence models for resistance calculations for AUVs with a typical Myring form using CFD. Their research involved resistance analyses of the three-dimensional viscous flows around various AUV models. The authors concluded that the SST k-ω turbulence algorithm is the most appropriate approach for estimating the hydrodynamic resistance of AUV models in such applications.

In a study by Joung et al. [11], a procedure was presented in which CFD analysis was used to determine the hull resistance of an AUV under development within a specific speed range. The results of the numerical analysis included the distributions of the velocity and pressure fields on the hull and propeller. Furthermore, a method was proposed for optimising the AUV's design to reduce the total resistance.

Allotta et al. [12] emphasised the need to develop an AUV that includes the typical features of a remotely operated vehicle (ROV), such as high manoeuvrability, while also possessing the essential characteristics of an AUV. The main objectives of this project included conducting search and surveillance tasks, managing and controlling fleets of vehicles, facilitating mutual localisation, and optimising communication between the vehicles. This study primarily discussed data that consisted of pre-simulations and tests conducted in a laboratory at various design stages before a sea trial of the vehicle. In a subsequent study, Allotta et al. [13] focused on the methodologies used in designing AUVs. They outlined the preliminary design criteria for these vehicles and described the design procedures, including testing of their drive systems. The THESAURUS project specified that an AUV should be designed with low viscous resistance, high manoeuvrability, and strong navigational capabilities, to achieve the expected level of performance.

Won et al. [14] aimed to identify the optimal geometric parameters for various forms of AUVs using CFD simulations. Their research focused on analysing the factors that influence the resistance force and propeller performance of AUVs, with a view to enhancing the efficiency of their propulsion systems. They applied the Taguchi method to improve the performance of the numerical analyses. In a separate study, Sousa et al. [15] investigated the turbulent flow around different geometric configurations of an AUV hull; their objective was to find a hull design that significantly reduced the energy consumption, thereby increasing the vehicle's operational autonomy.

Liu and Huang [1] presented extensive experimental measurements of the flow fields around an axially symmetrical hull, both with and without appendages. These measurements were taken at the Carderock Division Naval Surface Warfare Center and the Tracor Hydronautics Ship Model Basin. The purpose of their work was to use the experimental data obtained in this way to validate CFD models and other analyses related to submarine flow fields. Their database has been referenced in numerous scientific articles.

Budak and Beji [16] examined the resistance values for the bare hull form of the DARPA (Defense Advanced Research Projects Agency) Suboff submarine, along with several variants derived from this form. They used the SST *k-w* turbulence algorithm within the commercial CFD code ANSYS-FLUENT, and RANS calculations were carried out using the DARPA Suboff submarine model. The results were compared with experimental data. These researchers created three slightly different bow geometries and three stern geometries based on the generic DARPA Suboff bare hull, resulting in a total of nine new submarine forms. Numerical resistance calculations were performed for these newly developed geometric variants, and the results were used to identify the form variant with the lowest resistance, thus demonstrating that the proposed method could effectively generate a range of forms from a generic model to achieve a successful design with minimal viscous resistance.

Takahashi and Sahoo [17] conducted a detailed study of the DARPA Suboff model, using this as a benchmark due to the availability of experimental data for validation. These authors verified results related to the straight-ahead resistance, the other forces, and the moments acting on the hull during steady translation and turning with a drift angle. They validated various configurations at different speeds at the model scale, following a published methodology and procedure.

Elsamadisy et al. [18] discussed the use of biomimicry as an adaptive approach for developing new technological solutions inspired by nature. This method can enhance the environmental adaptation capabilities of various technological systems. Yu et al. [19] explained the mechanisms behind natural drag reduction and how the corresponding biomimetic strategies can be translated from nature into artificial functional surfaces.

El Daou et al. [20] explored the modelling, design, and fabrication of a bio-inspired robot that resembled a fish and was propelled by a flexible body. In a study by Honaryar and Ghiasi [21], the hydrodynamic characteristics and body shape of the catfish, *Hypostomus,* were exploited to design and develop an AUV called ZRAUV, which was intended to inspect subsea pipelines and cables. Göksu et al. [22] developed a bio-inspired hull form that exhibited reduced resistance compared to the DARPA Suboff, inspired by the body forms of predatory fish such as a barracuda, dorado, little tunny, and sailfish.

In their research on the propulsion of AUVs, Piskur et al. [23] investigated the thrust produced by a fin, and found that the generated force was influenced by both the flexibility of the fin and the frequency of its oscillation. They also highlighted the importance of accounting for fluid viscosity, especially in regard to the results obtained for a rigid fin. Zhao et al. [24] developed a novel hierarchical model with a leader to enhance the navigation of a swarm of underwater robots, inspired by the collective behaviours observed in natural animal groups such as shoals of fish and flocks of birds. In his investigation of a navigational system designed for a real biomimetic AUV, Praczyk [25] described simulation tests that were conducted to identify the most effective method for correcting a dead reckoning navigational system.

The aim of the present study is to develop a form for an AUV that minimises viscous resistance during forward movement. This vehicle is designed to dive to depths of 1,000 m and to cruise at a maximum speed of 10 knots. Its primary purpose is to conduct oceanographic, geological, and geophysical research in the Aegean Sea. Before conducting CFD analyses of the proposed AUV designs to estimate the hull resistance, numerical analyses are performed using the DARPA Suboff submarine model to validate the turbulence algorithms, discretisation methods, and boundary conditions that are employed in the subsequent analyses. The results obtained from this study are consistent with those of the well-known study by Liu and Huang [1]. The analyses are carried out using the commercial software STAR CCM+ (Simulation of Turbulent Flow in Arbitrary Regions - Computational Continuity Mechanics, C++ based). Following this, various AUV forms are created based on different torpedo shapes and Myring forms; AUV designs are also created through the application of the biomimicry principles discussed in Primrose's book [26] on the subject, which describes the application of biomimicry and biomimetics across various scientific fields. All of the generated designs are numerically analysed under the same conditions to determine the most suitable design form.

MATERIALS AND METHOD

The cruising range of an AUV is primarily determined by its battery capacity, and vice versa. The operating depth influences the strength requirements for the AUV, while the range of sensors and equipment to be carried determines its internal volume. Although several methods can be employed to develop the form and volume of an AUV, the most effective approach is often to consider existing AUVs or submarines along with their available test results. As Joubert [4] noted in his book, neglecting to take into account prior scientific studies would be a significant mistake when making any future changes to submarine designs. Alterations to a single component in a design can also necessitate modifications to all related features to ensure a functional design. In this context, biomimicry methodology presents an alternative and often more effective option for completing a design process.

In this study, we explore the development of an appropriate form for an AUV using biomimicry methods. The core idea behind biomimicry is to draw inspiration from the solutions that animals, plants, and organisms have evolved to address the challenges of their natural environments. Although this study focuses solely on the form design of an AUV, it can be interpreted more broadly as offering effective innovations for nearly every stage of the design process. Biomimicry is essentially a new science that involves examining not only the models found in nature but also the natural systems, processes, and elements that can provide solutions to various problems [27]. The aspects that set biomimicry apart from other design approaches are its emphasis on functionality and emulation of the solution methods that living systems have developed to overcome specific challenges. In contrast, biomorphic and bio-use-based designs tend to prioritise aesthetic considerations or practical applications derived from our fondness for natural forms. The distinctions between these approaches are illustrated in Fig. 1.

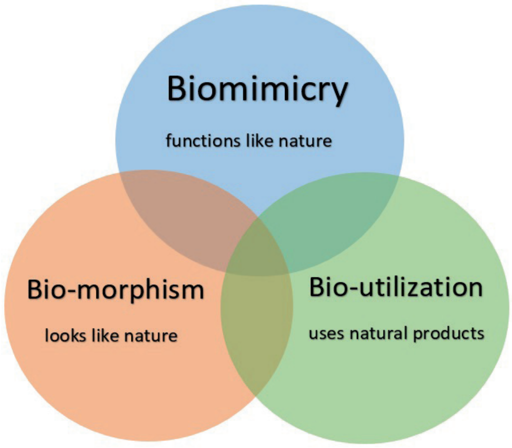

Fig. 1. Relationship between biomimicry, biomorphism, and bio-use [28]

Living organisms and natural systems are shaped by the mechanism of evolution to develop functional solutions to challenges. It is important to note that evolution does not create designs; instead, successful variations survive through natural selection and pass their functional advantages to future generations. Hence, contrary to popular belief, evolution does not imply "progress" or "development," as it is a process in which some variations resulting from mutations are filtered out by natural selection, allowing only those individuals with functional success to persist. In this context, while biomimicry design differs from traditional engineering design, a biomimicry design spiral can emerge if the fundamental stages of design activities are addressed from a unique perspective (Fig. 2).

The following explanations should be considered as the concluding statement for this concept. In his article, Banger defines the concept of biomimicry as follows: "Biomimicry examines the functioning, models, systems, processes, and components of nature to derive inspiration (and sometimes direct imitation) for solving engineering problems. Through these investigations, it aims to discover clues for innovative solutions. To put it in literary terms, biomimicry is the science of exploring the systematic workings of nature" [29]. Some sources differentiate between the concepts of biomimicry and biomimetics; although both fields use similar terms, definitions, and tools, the key distinction is that biomimicry is specifically used as a design concept [30].

In the present study, a biomimicry design approach is employed to enhance the hydrodynamic performance of unmanned and autonomous underwater vehicles. This strategy involves evaluating the forms of various sea creatures to align them with the functional requirements of the design. Based on this analysis, digital models of all the developed designs are created, and their hydrodynamic properties are thoroughly analysed. After examining the results, we determine the final design of an autonomous underwater vehicle that features the optimal characteristics.

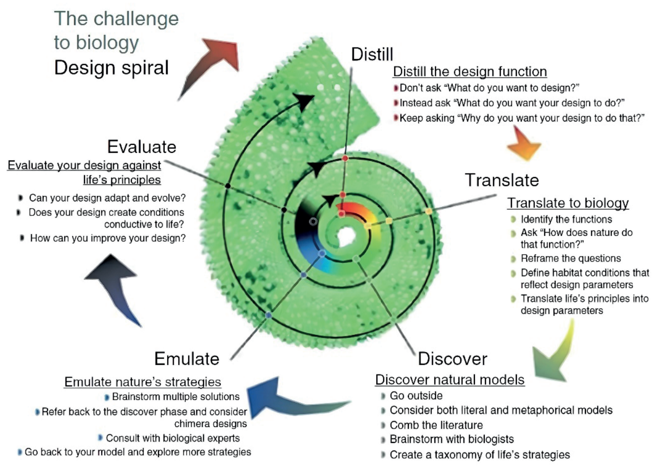

Fig. 2. Biomimicry design spiral [26]

The AUV should be designed to possess a high manoeuvrability capacity, similar to that of a remotely operated vehicle (ROV), while also retaining the typical characteristics of an AUV [12]. Moving objects submerged in a viscous fluid experience viscous drag, consisting of viscous pressure and frictional resistance, which depend on the Reynolds number. As a result, AUVs subjected to both frictional and viscous pressure resistances must have favourable hydrodynamic shapes and surface characteristics. In addition, these vehicles need to withstand high hydrostatic pressure forces on their structures, with the ranges depending on the demands of the tasks they will undertake in deep water.

Test results for the DARPA Suboff submarine are frequently used to validate the results of CFD analyses conducted for the design of submarine boats and AUVs. These results are also used to confirm the numerical results from all of the simulations undertaken in this study (Figs. 3 and 4). The DARPA submarine has a typical AUV form, and reliable test results are available for its performance. Hence, a model of this submarine was created and analysed in this study using STAR-CCM+ software (Figs. 4–7). Fig. 4 displays the model of the DARPA Suboff submarine, while Figs. 5 and 6 show the analysed domain and the meshed model, respectively. From Fig. 7, it can be seen that the results of the CFD analysis obtained in this study are aligned with the experimental results from submarine model tests conducted by Liu and Huang [1].

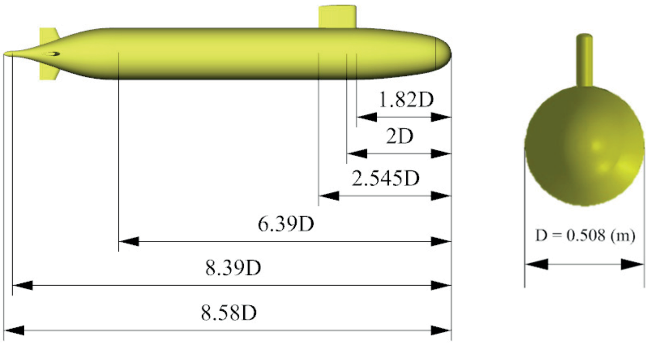

Fig. 3. DARPA SUBOFF submarine model [31]

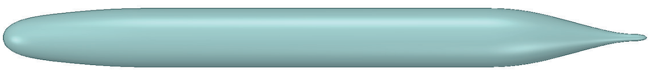

Fig. 4. Model of the DARPA SUBOFF submarine hull without appendages

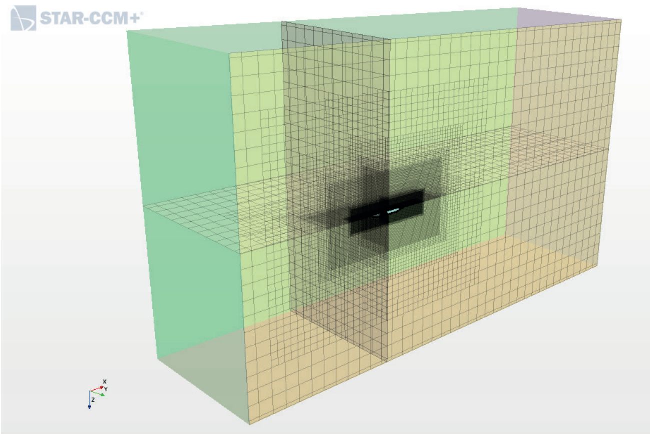

Fig. 5. Domain used for the DARPA Suboff submarine hull

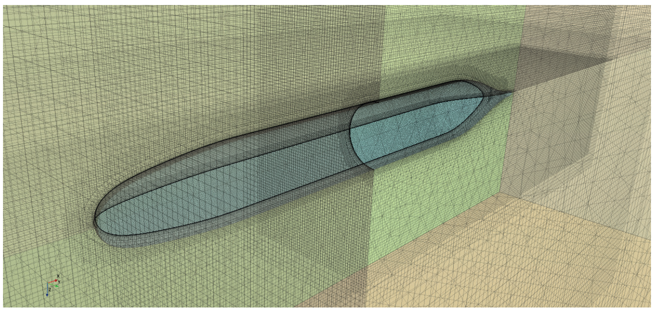

Fig. 6. Meshed model of the DARPA Suboff hull

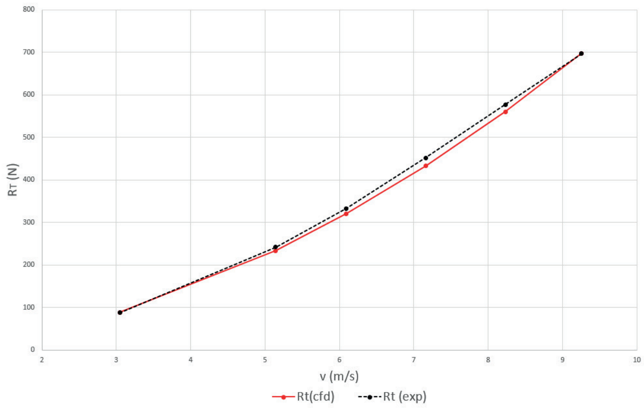

Fig. 7. Total resistance results from the test in [1] and our CFD analysis of the DARPA Suboff submarine model

In this study, we applied the methodology of biomimicry to create models based on the mature goose-beaked whale (*Ziphius cavirostris*), the mature sperm whale (*Physeter macrocephalus*), and the mature submarine shark (*Carcharodon carcharias*). These species were chosen because they possess the most efficient hydrodynamic forms, shaped by millions of years of evolution, and have the remarkable ability to dive to depths of up to 3,000 m, as illustrated in Figs. 8–11. Notably, beaked whales can reach top speeds of 11–12 km/h when submerged, while sperm whales can attain speeds of 35–45 km/h, and submarine sharks can reach speeds of 56 km/h underwater [32], [33]. We also developed three torpedo-shaped AUV models, a model of the Myring type, and four hybrid models incorporating the principles of biomimicry (Fig. 12). Each of these models had a volume displacement of approximately 5 m^3. All CFD analyses of the models were conducted in detail using the commercial software STAR CCM+ (Table 1). When all of the models had been created, their mesh structures were finalised as shown in Figs. 13–15.

Figs. 13–15 display all the created and meshed models of the whales, shark, and various AUVs, along with the domains in which these models were analysed. This procedural method facilitated a hydrodynamic comparison of the effectiveness of AUV designs based on torpedo shapes, two whale forms and a shark; these were all inspired by biomimicry, using their shapes that have evolved over millions of years. When comparing the torpedo-shaped and biomimicry-inspired AUV models, it is assumed that each will have a maximum speed of 5 m/s (18 km/h or 9.72 knots).

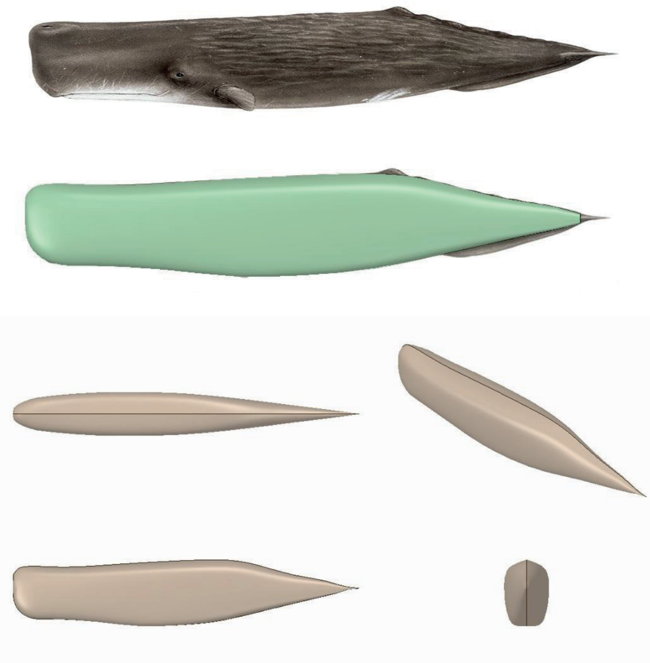

Fig 8. Modeling process of a mature sperm whale (Physeter macrocephalus)

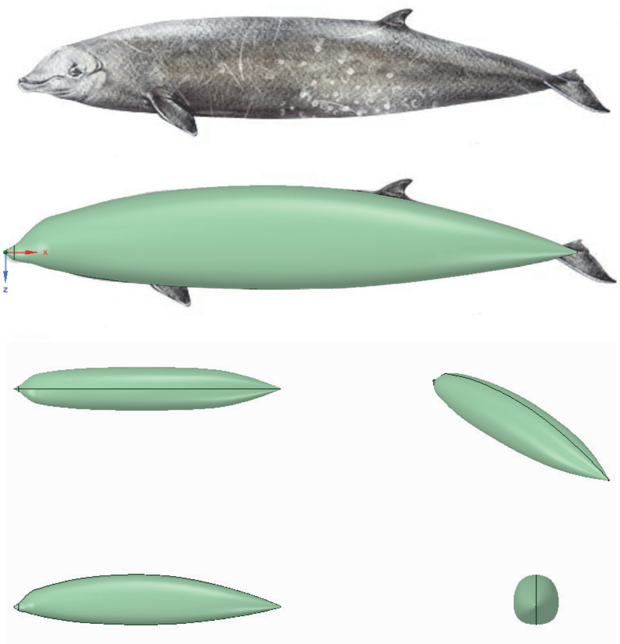

Fig. 9. Modeling process of a mature beaked whale (Ziphius Cavirostris)

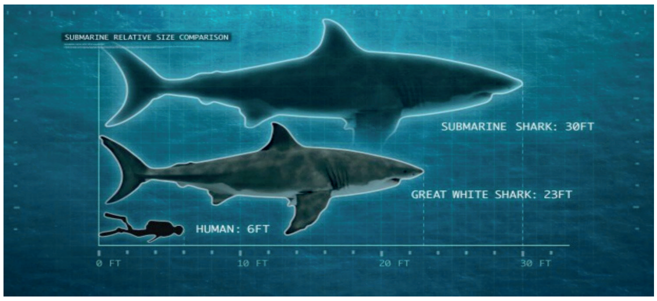

Fig. 10. Comparison showing the size of the submarine shark (Carcharodon carcharias) [36]

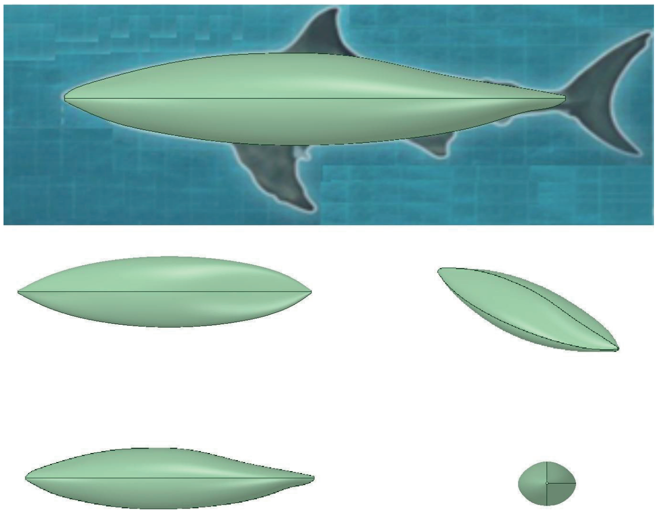

Fig. 11. Modelling process of a mature submarine shark (Carcharodon carcharias)

AUV-0 was developed based on the Myring form, which is commonly used for designing AUVs and predicting their viscous resistance levels (Fig. 12). Two additional AUV forms were modelled based on a torpedo shape for analysis under the same conditions: one featured a spherical head and is referred to here as AUV-1, while the other had an ellipsoid head with a relatively slender stern, which is designated as AUV-2 (Fig. 12). The parallel hull of AUV-2 and its stern were also removed, and the ellipsoid head of the hull was then combined with an elongated, arrow-like stern, resulting in a new design called AUV-3 (Fig. 12). The purpose of creating this new form was to significantly reduce the resistance observed for AUV-1 and AUV-2.

Due to the small volume displacement of AUV-3 relative to its length, hybrid models were proposed using a biomimicry methodology, denoted here as AUV-4 through AUV-7. All underwater vehicles are designed with positive buoyancy, meaning they have a lifting force that allows them to surface when their energy is depleted or if their systems fail due to any electromechanical issues. For this reason, vertical-axis motors and propellers are needed to maintain a constant depth in the sea. However, this requirement leads to an evident increase in energy consumption, which can limit the duration of underwater operations.

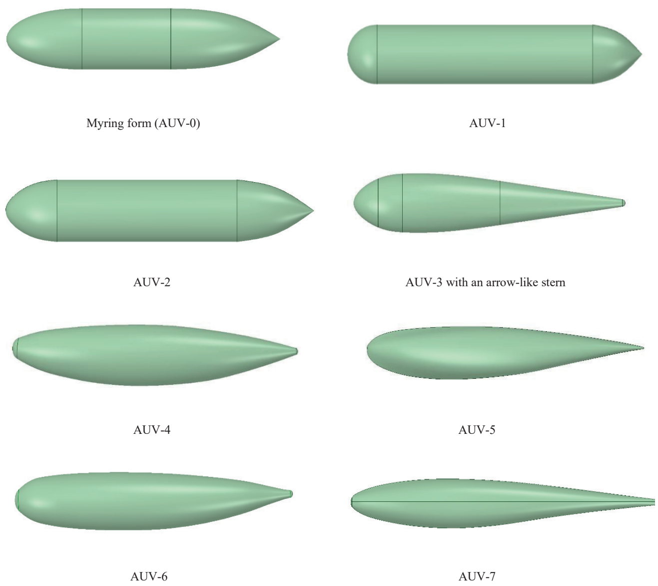

Fig. 12. Creation of torpedo-shaped and bio-inspired hybrid models

To address this challenge, the designs of AUV-4, AUV-5, AUV-6, and AUV-7 were inspired by the shape of a "spoiler," and mimicked the forms of a beaked whale, a sperm whale, and a submarine shark as an "inverted wing". This design generates downward thrust during constant forward motion, allowing the AUVs to achieve neutral buoyancy and reducing the energy consumption (Fig. 12). The manufacturing process for these last four models was simpler than for the beaked whale, sperm whale, and submarine shark models.

The bow of the AUV-4 model was based on AUV-3, while its middle body and stern were inspired by the form of a beaked whale, and the whole body was rotated 180° around the longitudinal axis according to the biomimicry principle, as shown in Figs. 9 and 12. This design allowed the AUV-4 to take on a spoiler shape, thus reducing the need for downward thrust during constant forward movement by creating a rising negative pressure field beneath the vehicle. The design of AUV-5 was derived from both a mature beaked whale and a sperm whale, and was also rotated 180° around the longitudinal axis, following the biomimicry principle, as illustrated in Figs. 8, 9, and 12. The sperm whale model was modified with a completely altered head shape, and this was designated as AUV-6 (Fig. 12).

The final hybrid model, AUV-7, was inspired by a mature beaked whale, and was rotated 180° around the longitudinal axis. This design was adapted to incorporate the features of a mature submarine shark. The unique characteristics of the AUV-7 model were patented by the Turkish Patent and Trademark Office in 2021, and have been submitted to the Patent Cooperation Treaty for protection. Table 1 provides a comprehensive overview of all the models developed in this study, and Figs. 13–15 show the meshed models for all the AUVs.

Tab. 1. Origins of the models

Name of model	Models	Configuration
Beaked whale	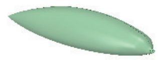	Model of a goose-beaked whale
Sperm whale		Model of a sperm whale
Submarine shark		Model of a submarine shark
AUV-0 (Myring)	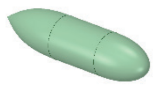	Myring model based on the original equation
AUV-1	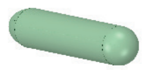	Torpedo-shaped model with a hemispherical head
AUV-2	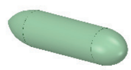	Torpedo-shaped model with ellipsoid head and slender stern
AUV-3	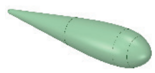	Torpedo-shaped model with an ellipsoid head and an arrow-like stern
AUV-4		Model based on a mature beaked whale with an ellipsoid head, rotated 180° around the longitudinal axis
AUV-5	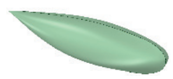	Hybrid model inspired by a beaked whale and a sperm whale, rotated 180° around the longitudinal axis
AUV-6	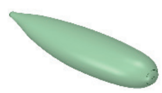	Model of a mature sperm whale with a modified head shape
AUV-7	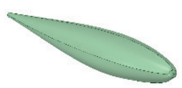	Hybrid model inspired by a beaked whale, rotated 180° around the longitudinal axis and modified based on the form of a submarine shark

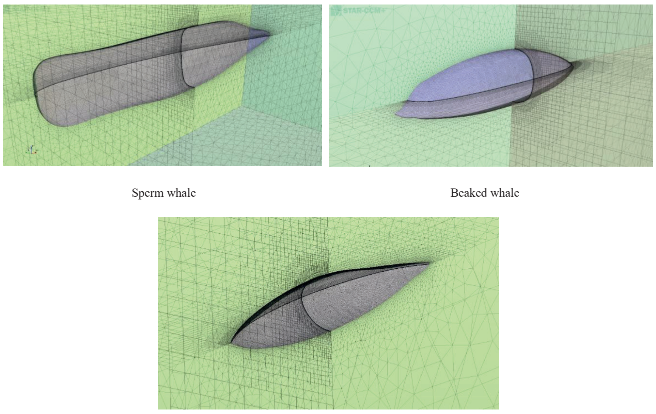

Sperm whale

Beaked whale

Submarine shark

Fig. 13. Meshed models of three sea creatures

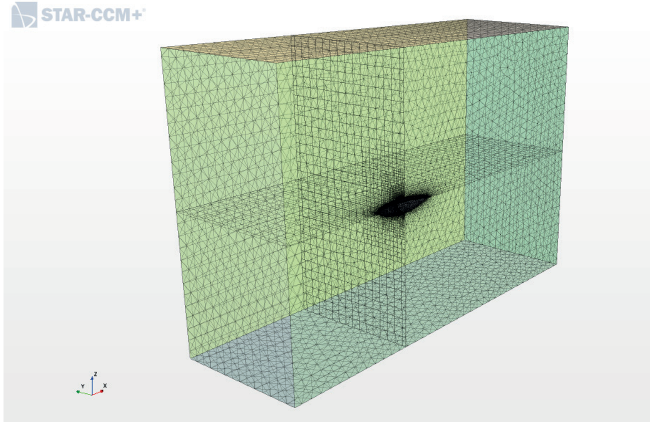

Fig. 14. Domain for a meshed model (domains for all models are similar)

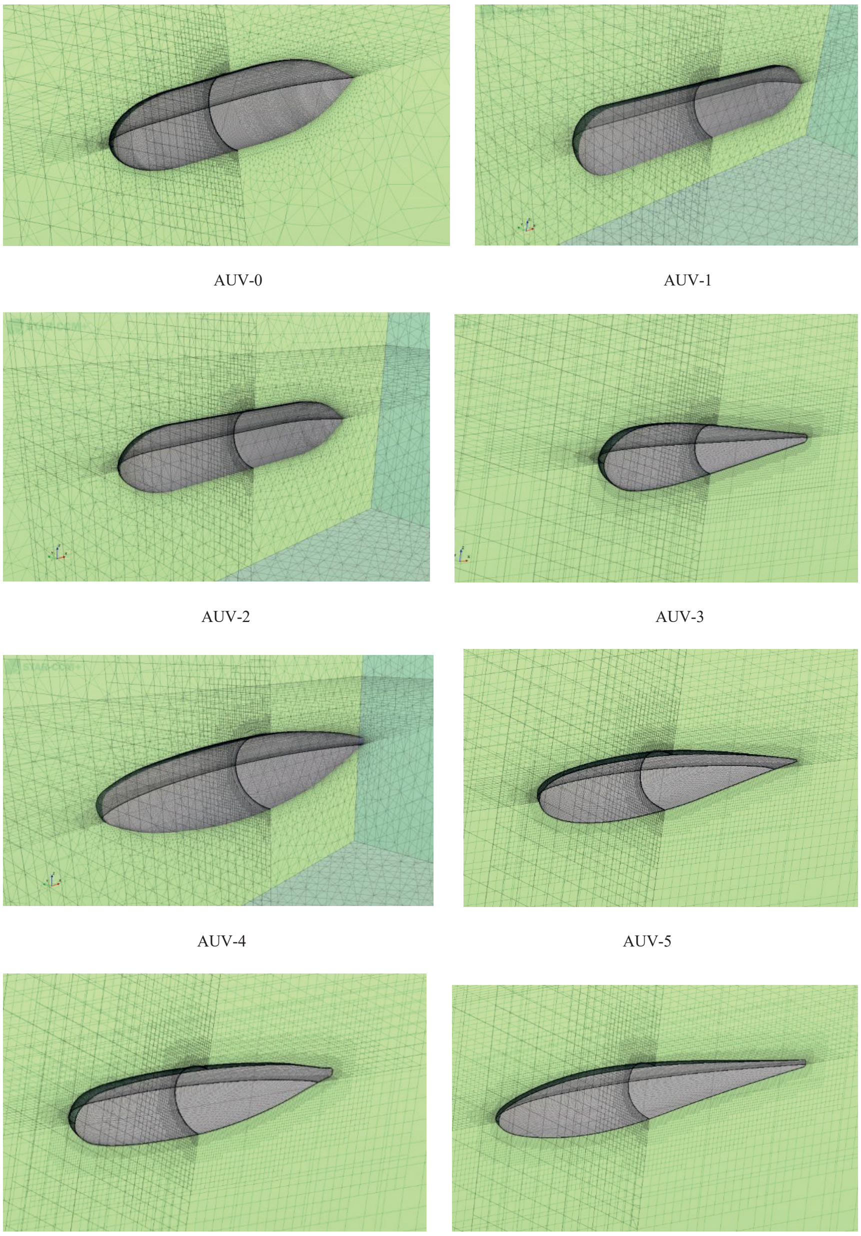

AUV-0

AUV-1

AUV-2

AUV-3

AUV-4

AUV-5

AUV-6

AUV-7

Fig. 15. Meshed models of AUV-0 to AUV-7

ANALYSIS OF THE MODELS AND RESULTS

BACKGROUND: CFD METHOD AND TURBULENCE MODEL

In this study, we examined the hydrodynamic properties of the developed AUVs using the commercial CFD solver STAR CCM+. This solver employs the Navier-Stokes equations, which describe the turbulent viscous flows around floating and submerged hulls. Due to the chaotic nature of the turbulence in fluid flow, it is necessary to use time-averaged values of the flow parameters using an approach known as the RANS equations. The continuity and momentum equations must also be developed for an incompressible Newtonian fluid, as shown in Eqs. (1) and (2), respectively.

$$\nabla \cdot \overline{\boldsymbol{u}} = 0 \tag{1}$$

$$\rho \frac{\partial \overline{\boldsymbol{u}}}{\partial t} + \rho(\overline{\boldsymbol{u}} + \nabla \overline{\boldsymbol{u}}) = \rho \boldsymbol{g} - \nabla \overline{\boldsymbol{p}} + \mu \nabla^2 \overline{\boldsymbol{u}} + \nabla \cdot \boldsymbol{T}_R \tag{2}$$

where $\overline{\boldsymbol{u}}$ and $\overline{\boldsymbol{p}}$ denote the average velocity and pressure fields, respectively, ρ is the density of the fluid, μ is its dynamic viscosity, and $\mathbf{T}_R$ is the tensor of Reynolds stresses. In this case, the flow around the AUV hulls was considered to be steady and incompressible. The energy equation is removed from the conservation equations for incompressible flow, leaving only the continuity and momentum equations.

To carry out CFD analyses of the AUV models discussed in the following section, we employed the SST *k-ω* (SSTKW) turbulence algorithm implemented in STAR-CCM+ software. This model was chosen because it typically provides an accurate estimate of the onset and extent of flow separation under reverse pressure gradients for both floating and submerged rigid vessels. The SSTKW algorithm features a modified turbulent viscosity formulation that is used to calculate the transport effects of the principal turbulent shear stress. It also includes a blending function that activates the standard *k-ω* algorithm in the near-wall region while a transformed *k-ε* algorithm is applied in the far-field zones ([34], [35]). The following two transport equations are used to calculate the turbulence kinetic energy (*k*) and the specific dissipation rate (*ω*) (Eqs. (3) and (4)).

$$\frac{\partial}{\partial t}(\rho k) + \frac{\partial}{\partial x_i}(\rho k u_i) = \frac{\partial}{\partial x_j}\left(\Gamma_k \frac{\partial k}{\partial x_j}\right) + G_k - Y_k + S_k \tag{3}$$

$$\frac{\partial}{\partial t}(\rho \omega) + \frac{\partial}{\partial x_i}(\rho \omega u_i) = \frac{\partial}{\partial x_j}\left(\Gamma_\omega \frac{\partial \omega}{\partial x_j}\right) + G_\omega - Y_\omega + D_\omega + S_\omega \tag{4}$$

where G_k and G_ω denote the generation of turbulence kinetic energy and the generation of specific dissipation rate, respectively; Γ_k and Γ_ω are the effective diffusivity of *k* and *ω*, respectively; S_k and S_ω represent user-defined source terms; Y_k and Y_ω denote the dissipation of *k* and *ω* due to turbulence, respectively, and D_ω is the cross-diffusion term.

The mesh elements surrounding the AUV hulls and within the domain were generated according to the chosen turbulence model. To achieve more reliable results, a layered mesh structure was created near the surfaces of the AUV hulls, using a trimmed hexahedral cell shape-based core mesh. In the outer region of the domain, a larger mesh grid of the same type was used (Figs. 13–15). It is important to note that the selected turbulence algorithms typically operate within a specific range of the wall function y^+, as shown in Eq. (5).

$$y^+ = \frac{\rho y \sqrt{\frac{\mu}{\rho}\left(\frac{\partial u}{\partial y}\right)_{y=0}}}{\mu} \tag{5}$$

Figs. 14 and 16 show the grid structure for the entire fluid domain, along with the distributions of the y^+ values obtained during the resistance analysis of the DARPA Suboff model. The range of variation in the y^+ values for the wall function within the boundary layer of the DARPA Suboff submarine hull and for the other generated models is shown in Figs. 16 and 17 for a velocity of 5 m/s. The y^+ values for these models ranged from zero to one. These results indicate that an excellent outcome was achieved in terms of the boundary layer modeling quality. The results of the resistance simulation in this study were validated against data from towing tank tests of the DARPA Suboff model conducted by Liu and Huang [1], as shown in Fig. 7.

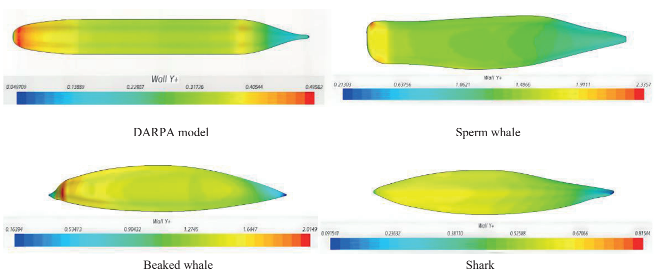

Fig. 16. y^+ distributions for the DARPA model and the models based on sea creatures

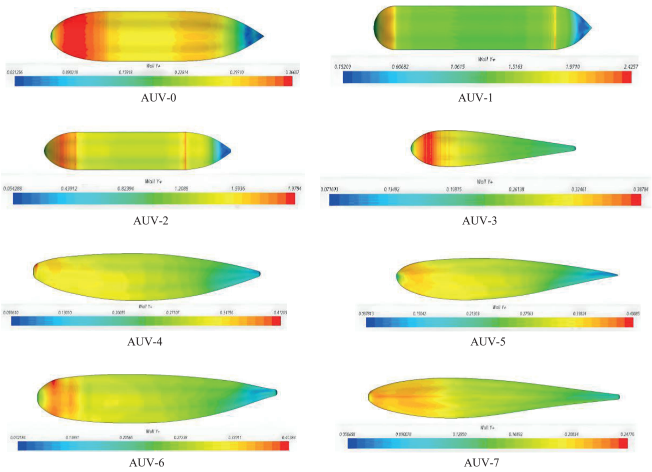

Fig. 17. y^+ distributions for models AUV-0 to AUV-7

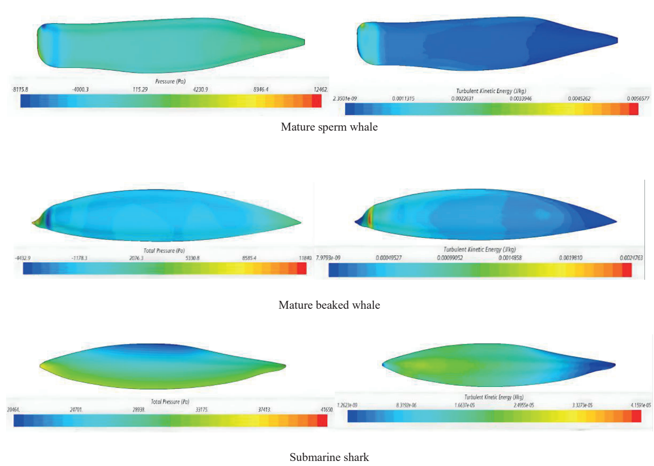

Fig. 18. Total pressure and turbulent kinetic energy distributions for the models based on sea creatures

ANALYSIS OF THE DEVELOPED MODELS

In this section, we numerically analyse all 11 models after successfully verifying the CFD simulations of the DARPA Suboff submarine model against the test results published by Liu and Huang [1]. The analysis of these models was conducted using the SST k–ω turbulence algorithm (SSTKW-Menter) in STAR-CCM+ software (Figs. 18–22).

When evaluating the values for the total viscous resistance of the whales and the shark obtained from the numerical analysis, several noteworthy observations emerged. Despite the differences in the forms of the whales and the shark, all three species had nearly identical viscous resistance values when fully submerged (Figs. 18 and 21). This similarity is attributed to the comparable pressure and turbulent kinetic energy distribution fields on their hull surfaces, as shown in Fig. 18.

The results of the resistance simulations for AUV-1 were significantly higher than for the other AUVs and models of sea creatures (Figs. 18–21). This is likely to be because AUV-1 generates a higher level of turbulent kinetic energy. In contrast, AUV-7 and the models based on sea creatures had between 1.5% and 14% less friction and viscous pressure resistance compared to AUV-2 to AUV-6 and AUV-0 (Fig. 21). The turbulent kinetic energy distribution fields of these models vary at the sterns due to differences in turbulence levels; however, AUV-7 and the models based on sea creatures have more uniform fields than AUV-1 and the other AUVs (Figs. 18–22).

The total resistance values for the designs of AUV-2 and AUV-3 were reduced by approximately 15% and 15.5%, respectively, compared to AUV-1. The distribution fields of the pressure and turbulent kinetic energy for AUV-2 and AUV-3 are also significantly better than for AUV-1, as illustrated in Figs. 17 and 19. The overall waterplane section area for the hypothetical form of AUV-3 resembles that of a ship's rudder (Fig. 19) and generates considerably less turbulence at the stern than that observed at the aft hulls of AUV-1 and AUV-2. However, the level of turbulence (and hence the viscous resistance) remains higher than for AUV-7, as well as for the two whale models and the shark, as depicted in Figs. 18–20. Despite this, the design of AUV-3 and the hybrid designs of AUV-4 to AUV-6 have similar total resistance values.

The biomimicry-inspired hybrid models, designated here as AUV-4 to AUV-7, were designed with four primary objectives. The primary goal was to create a form design with low viscous resistance, high propulsive efficiency, and excellent manoeuvrability. A secondary goal was the development of a spoiler form that could generate a negative pressure field beneath the vehicles during forward travel. This design reduces energy consumption by decreasing the reliance on vertical thrusters while forward cruising at constant speed and by minimising the longitudinal hydrodynamic resistance encountered. The internal capacity of these models could also be increased to accommodate various devices and equipment. Lastly, the manufacturing process for these models was designed to be simpler and more cost-effective compared to the models of the sea creatures from which all the designs drew inspiration.

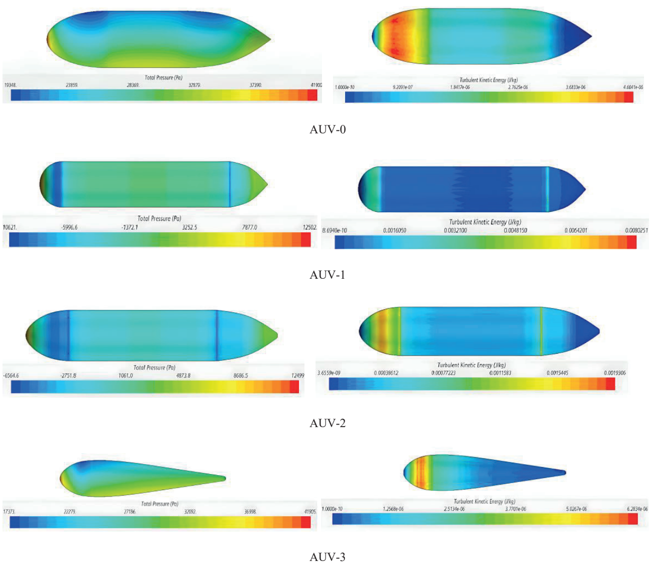

Fig. 19. Total pressure and turbulent kinetic energy distributions for the torpedo-shaped models AUV-0 to AUV-3

The pressure distribution fields on the hybrid forms of AUV-4 to AUV-7 appear significantly more asymmetrical than for AUV-0-3. This difference arises from the "spoiler" features on AUV-4 to AUV-7, as illustrated in Figs. 19–20, which generate downward forces to counteract the vehicle's positive buoyancy while moving forward at constant speeds of between 1 and 5 m/s (Fig. 22). Consequently, AUV-4 to AUV-7 can achieve notable energy savings in applications where the vehicles' forward motion is constant. In view of these factors and the results of the simulations conducted in this study, the advantages of the AUV-7 become particularly clear, which stem from the degree of its positive buoyancy and its constant forward speed (Figs. 21 and 22).

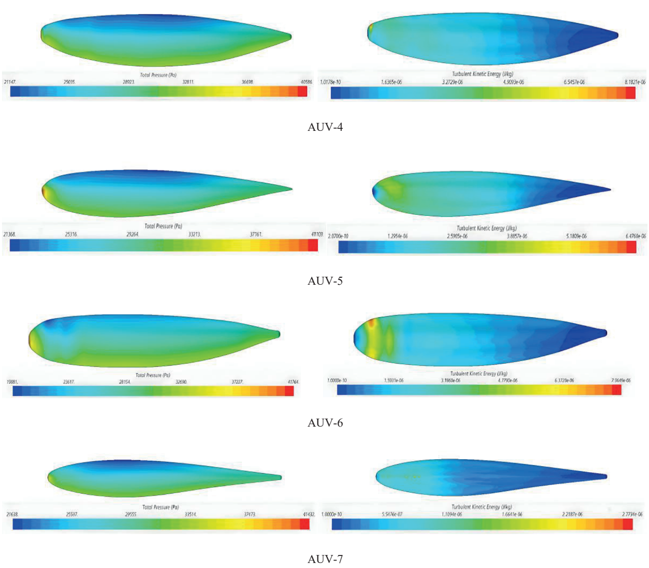

Fig. 20. Total pressure and turbulent kinetic energy distributions for the bio-inspired models AUV-4 to AUV-7

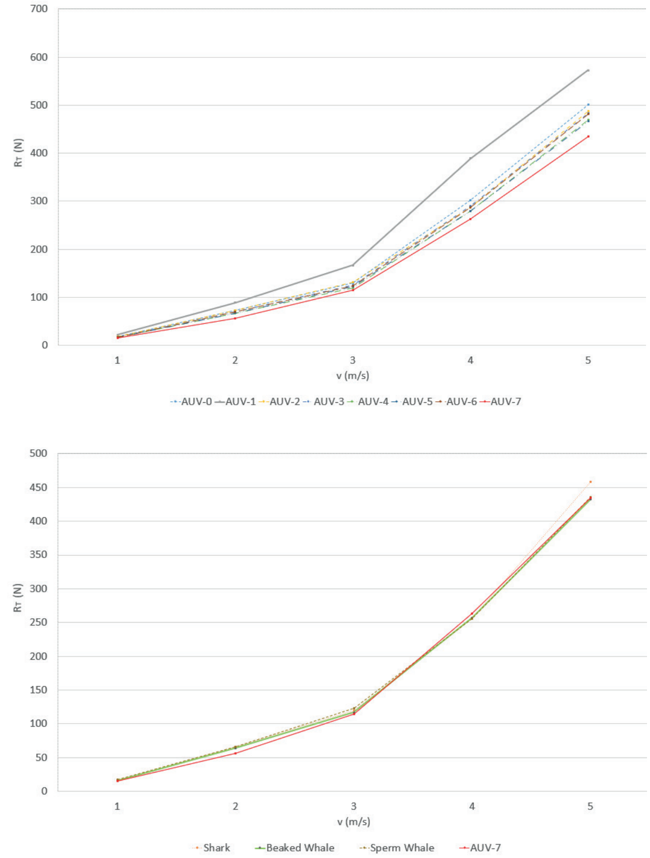

Fig. 21. Total resistance results from the CFD analyses of all models

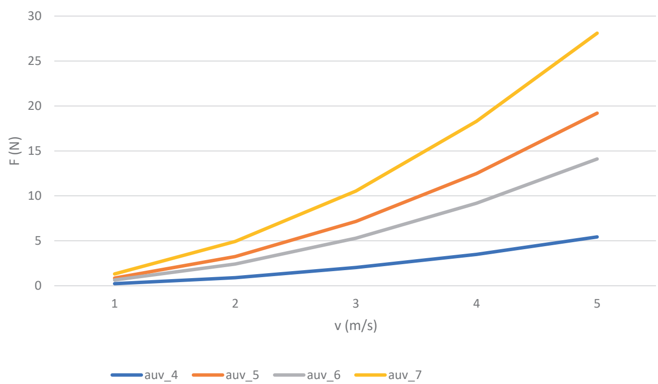

Fig. 22. Negative buoyancy force for AUV-4 to AUV-7

Tab. 2. Negative buoyancy force for AUV-4 to AUV-7 in relation to resistance

	AUV-0	AUV-1	AUV-2	AUV-3	AUV-4	AUV-5	AUV-6	AUV-7
F_{sbmrg} (N) $v = 5$ m/s	0	0	0	0	5.43	19.2	14.1	28.1
F_{sbmrg}/R_T	0	0	0	0	0.01157	0.04120	0.02925	0.06459

CONCLUSION

This study aimed to develop an appropriate design form for an AUV that was intended to explore the geological and geophysical characteristics of the seabed and to conduct oceanographic research.

To achieve this, the DARPA Suboff submarine model was initially analysed to verify the results of the numerical simulations conducted in this study using the CFD method. These numerical simulation results were validated against test data from the DARPA Suboff model. We also used biomimicry as a novel design method. A biomimicry approach entails studying the functions, models, systems, processes, and components that arise in nature for inspiration (and sometimes direct imitation) in order to address engineering challenges. As an emerging science, this approach emphasises functionality and emulation of the solutions that living systems have developed to overcome specific problems. In this context, comprehensive simulations were carried out in the same manner using the commercial software STAR CCM+ on models created with the same volume displacement and similar aspect ratios, based on the following forms:

- a mature goose-beaked whale (*Ziphius cavirostris)*,
- a mature sperm whale (*Physeter macrocephalus*),
- a mature submarine shark (*Carcharodon carcharias*)
- four torpedo-shaped AUV models that are frequently used
- four AUV models inspired by biomimicry.

The results are discussed in detail below.

The hybrid models AUV-4 through AUV-7 were designed with four primary objectives. The primary goal was to create a design with low viscous resistance, high propulsive efficiency, and excellent manoeuvrability. Since these AUVs are designed with positive buoyancy, they can surface quickly in the event of any electromechanical failure. A second goal involved incorporating a "spoiler" profile into biomimicry-inspired shapes to minimise the energy consumption during forward travel at a constant speed, thereby allowing the AUV to maintain a constant depth. Thirdly, the vehicle was required to have a spacious design in order to accommodate various devices and equipment. Lastly, this design had to be simple and cost-effective to ensure low production costs.

The designs for AUV-4 to AUV-7 developed in this study have superior resistance properties compared to the AUV-0 and AUV-1 models, particularly in regard to the turbulent kinetic energy distribution fields. The resistance values for the bio-inspired hybrid forms (AUV-4 to AUV-6) are similar only to those of the torpedo-shaped forms (AUV-2 and AUV-3). The analysis results for the forms of AUV-4 to AUV-6 are notably similar to each other. In addition, both the whale and shark forms, based on shapes that have evolved over millions of years, have superior hydrodynamic characteristics compared to AUV-0, AUV-1, AUV-2, and AUV-3. The hydrodynamic properties of these creatures closely resemble those of AUV-4 to AUV-7, with AUV-7 exhibiting the lowest resistance values.

When designing AUVs with positive buoyancy that will surface in the event of electromechanical failure, it should be noted that the closer the vehicle's positive buoyancy to its neutral buoyancy state, the less its operation depends on vertical thrusters. AUV-7, with its unique configuration, generates the maximum negative buoyancy force of 28.1 N of the bio-inspired AUVs considered here, while producing the least resistance force of 430 N of all the AUVs, as shown in Table 2 and Figs. 21 and 22. This setup can achieve a certain amount of energy saving while maintaining a constant forward speed of 5 m/s, which is particularly beneficial for underwater scanning operations that are typically conducted at this constant speed.

The development of an AUV with the lowest possible resistance characteristics and energy consumption is a key design priority. However, it is essential to ensure that there is sufficient interior space to accommodate the navigation, propulsion systems, and other necessary equipment. Forms based on sea creatures have significantly less internal volume and incur higher production costs compared to the designs of AUV-4 to AUV-7. The patented design of AUV-7 was therefore selected as the final design; this form offers several advantages, including minimal viscous resistance, maximum downward forces during forward travel at a constant speed, cost-effective production, and more space for batteries, navigation, propulsion, measurement systems, and other equipment compared to the other AUVs examined here.

Future research should focus on the propulsion and manoeuvrability of the bio-inspired forms, particularly AUV-7, under disturbance conditions such as water currents and variable buoyancy. This will help to create very reliable designs.

REFERENCES

1. Liu H L, Huang TT. Summary of DARPA SUBOFF experimental program data. Naval Surface Warfare Center Carderock Div Bethesda Md Hydromechanics Directorate, 1998.

2. Gürsel KT,Taner M, Ünsalan D, Neşer G, Altunsaray E, Önal M. Form development and validation of an autonomous underwater vehicle, "Mircea cel Batran" Naval Academy Scientific Bulletin SBNA 2017, vol. XX, no. 1.

3. Myring DF. A theoretical study of body drag in subcritical axisymmetric flow. Aeronautical Quarterly 1976, vol. 27, no. 3, pp. 186–194. https://doi.org/10.1017/S000192590000768X

4. Joubert P. Some aspects of submarine design, Part 1: Hydrodynamics, DSTO Platforms Sciences Laboratory, Australia, 2004.

5. Bertram V. Submarine hull design. Monograph on Submarine Design & Engineering in Department of Ocean Engineering, Indian Institute of Technology Madras, 2012.

6. Madhan R, Desa ES, Prabhudesai S, Sebastiao L, Pascoal A, Desa E, Mascarenhas AAMQ, Maurya P, Navelkar

GS, Afzulpurkar S, Khalap S. Mechanical design and development aspects of a small AUV-Maya. 7th IFAC Conference MCMC2006, 2006.

7. Joung T, Sammut K, He F, Lee S. A study on the design optimization of an AUV by using computational fluid dynamic analysis. Proceedings of the Nineteenth International Offshore and Polar Engineering Conference Osaka, Japan, June 21-26 2009. ISBN 978-1-880653-53-1 (Set); ISSN 1098-618. https://api.semanticscholar.org/CorpusID:9772684

8. Husaini M, Samad Z, Arshad M R. CFD simulation of cooperative AUV motion. Indian Journal of Marine Sciences IJMS 2009, vol. 38, no. 3, pp. 346-351.

9. Karim M, Rahman M, Alim A. Numerical computation of viscous drag for axisymmetric underwater vehicles. Jurnal Mekanikal 2008, no. 26, pp. 9–21. https://jurnalmekanikal.utm.my/index.php/jurnalmekanikal/article/view/135

10. Fangxi S, Lianhong Z, Zhiliang W, Leping W. On resistance calculation for autonomous underwater vehicles. Advanced Materials Research AMR 2011, vols. 189-193, pp. 1745–1748. https://doi. org/10.4028/www.scientific.net/AMR.189-193.1745

11. Joung TH, Sammut K, He F, Lee SK. Shape optimization of an autonomous underwater vehicle with a ducted propeller using computational fluid dynamics analysis. International Journal of Naval Architecture and Ocean Engineering IJNAOE 2012, vol. 4, pp. 44–56. https://doi.org/10.2478/IJNAOE-2013-0077

12. Allotta B, Pugi L, Bartolini F, Costanzi R, Ridolfi A, Monni N, Natalini M. The THESAURUS project, a long range AUV for extended exploration, surveilance and monitoring of archeological sites. V International Conference on Computational Methods in Marine Engineering ECCOMAS MARINE, 2013. http://hdl.handle.net/2117/333078

13. Allotta B, Pugi L, Bartolini F, Ridolfi A, Costanzi R, Monni N, Gelli J. Preliminary design and fast prototyping of an autonomous underwater vehicle propulsion system. Proceedings of the Institution of Mechanical Engineers Part M: Journal of Engineering for the Maritime Environment 2014, vol. 229, no. 3. pp. 248-272. https://doi.org/10.1177/1475090213514040

14. Won DJ, Kim J, Kim J. Design optimization of duct-type AUVs using CFD analysis. Intelligent Service Robotics 2015, vol. 8, no. 4, pp. 233–245. https://doi.org/10.1007/s11370-015-0179-9

15. Sousa JVN, Macêdo ARL, Junior WFA, Lima AGB. Numerical analysis of turbulent fluid flow and drag coefficient for optimizing the AUV hull design. Open Journal of Fluid Dynamics OJFD 2014, vol. 4, pp. 263–277. https://doi.org/10.1007/s11370-015-0179-910.4236/ojfd.2014.43020

16. Budak G, Beji S. Computational resistance analyses of a generic submarine hull form and its geometric variants. Journal of Ocean Technology JOT 2016, vol. 11, no. 2, pp. 77-86.

17. Takahashi K, Sahoo PK. Fundamental CFD Study on the hydrodynamic performance of the DARPA SUBOFF submarine. ASME 2019 38th International Conference on Ocean, Offshore and Arctic Engineering. American Society of Mechanical Engineers Digital Collection, 2019. https://doi.org/10.1115/OMAE2019-96190

18. Elsamadisy R, Sarhan AE, Farghaly Y, Mamdouh A. Biomimicry as a design approach for adaptation. J. Al-Azhar Univ. Eng. Sect. 2019, vol. 14, pp. 1516–1533. https://doi.org/10.21608/auej.2019.64210

19. Yu C, Liu M, Zhang C, Yan H, Zhang M, Wu Q, Liu M, Jiang L. Bio-inspired drag reduction: From nature organisms to artificial functional surfaces. Giant 2020, vol. 2, p. 100017. https://doi.org/10.1016/j. giant.2020.100017

20. El Daou H, Salumäe T, Toming G, Kruusmaa M. A bio-inspired compliant robotic fish: Design and experiments. IEEE International Conference on Robotics and Automation, 2012, pp. 5340–5345. https://doi. org/10.1109/ICRA.2012.6225321

21. Honaryar A, Ghiasi M. Design of a bio-inspired hull shape for an AUV from hydrodynamic stability point of view through experiment and numerical analysis. J. Bionic Eng. 2018, vol. 15, pp. 950–959. https://doi.org/10.1007/s42235-018-0083-z

22. Göksu B, Erginer KE, Öner G. Comparison of submarine hull morphologies obtained by biomimicry method with DARPA SUBOFF. Naval Engineers Journal NEJ 2024, vol. 136, no.3, pp. 87–104.

23. Piskur P, Szymak P, Kitowski Z, Flis L. Influence of fin's material capabilities on the propulsion system of biomimetic underwater vehicle. Polish Maritime Research PMR 2020, 4(108), vol. 27, pp. 179–185. https://doi.org/10.2478/pomr-2020-0078

24. Zhao Q, Yang T, Tang G, Yang Y, Luan Y, Wang T, Xu M, Li S, Xie G. Hierarchical Model for an AUV swarm with a leader. Polish Maritime Research PMR 2025, 1(125), vol. 32, pp. 71–80. https://doi.org/10.2478/pomr-2025-0007

25. Praczyk T. Correction of navigational information supplied to biomimetic autonomous underwater vehicle. Polish

Maritime Research PMR 2018, 1(97), vol. 25, pp. 13–23. https://doi.org/10.2478/pomr-2018-0002

26. Primrose SB. Biomimetics: Nature-inspired design and innovation. John Wiley & Sons; 2020.

27. Benyus JM. Biomimicry: Innovation inspired by nature. Morrow; 1997. ISBN 10: 0060533226 .

28. What is biomi micry? 17.08.2022. Retrieved from: https://biomimicry.org/what-is-biomimicry/

29. Genç M. Nature, art and biomimetical science. Doctor of Arts Degree, Hacettepe University, Graduate School of Fine Arts (in Turkish), 2013.

30. Kuday I. Examination of the concept of biomimicry as a supporting factor of the design process. Masters' thesis, Mimar Sinan Fine Arts University, Istanbul (in Turkish), 2009.

31. Lin YH, Li XC. The investigation of a sliding mesh model for hydrodynamic analysis of a SUBOFF model in turbulent flow fields. Journal of Marine Science and Engineering JMSE 2020, vol. 8, no. 10, p. 744. https://doi.org/10.3390/jmse8100744

32. Naughton D. The natural history of Canadian mammals, University of Toronto Press; 2020. ISBN 078-1-4426-4483-0.

33. Sperm whale. 14.03.2017. Retrieved from: https://oceanwide-expeditions.com/to-do/wildlife/spermwhale.

34. Menter F. Two-equation eddy-viscosity turbulence models for engineering applications. AIAA Journal 1994, vol. 32 no 8, pp. 1598–1605. https://doi.org/10.2514/3.12149

35. Gürsel KT, Taner M. Hydrodynamic potential improvement of pontoon boats. Naval Engineers Journal NEJ 2019, no. 131-2, pp. 105-112.

36. Shark of Darkness: Wrath of Submarine. 17.08.2022. Retrieved from: https://www.imdb.com/title/tt4177960/mediaviewer/rm2106087936/